

## Examining the impact of $\alpha$ -decay energies on the odd-even staggering in half-lives: $\alpha$ -decay spectroscopy of $^{207-209}\text{Ac}$

H. B. Yang (杨华彬)<sup>1,2</sup>, Z. G. Gan (甘再国)<sup>1,3,\*</sup>, Z. Y. Zhang (张志远)<sup>1,3</sup>, M. H. Huang (黄明辉)<sup>1,3</sup>, L. Ma (马龙)<sup>1,†</sup>, M. M. Zhang (张明明)<sup>1</sup>, C. L. Yang (杨春莉)<sup>1,3</sup>, Y. L. Tian (田玉林)<sup>1,3</sup>, Y. S. Wang (王永生)<sup>1,3,4</sup>, H. B. Zhou (周厚兵)<sup>5</sup>, X. J. Wen (温小江)<sup>5</sup>, J. G. Wang (王建国)<sup>1,3</sup>, Z. Zhao (赵圳)<sup>1,3</sup>, S. Y. Xu (徐苏扬)<sup>1,3</sup>, L. X. Chen (陈立欣)<sup>1,3</sup>, X. Y. Huang (黄鑫源)<sup>1,3</sup>, C. X. Yuan (袁岑溪)<sup>6</sup>, Y. F. Niu (牛一斐)<sup>4</sup>, H. R. Yang (杨贺润)<sup>1,3</sup>, W. X. Huang (黄文学)<sup>1,3</sup>, Z. Liu (刘忠)<sup>1,3</sup>, X. H. Zhou (周小红)<sup>1,3</sup>, Y. H. Zhang (张玉虎)<sup>1,3</sup>, S. G. Zhou (周善贵)<sup>7,3</sup>, Z. Z. Ren (任中洲)<sup>8</sup>, H. S. Xu (徐瑚珊)<sup>1,3</sup>, V. K. Utyonkov<sup>2</sup>, A. A. Voinov<sup>2</sup>, Yu. S. Tsyganov<sup>2</sup>, A. N. Polyakov<sup>2</sup> and D. I. Solov'ev<sup>2</sup>

<sup>1</sup>*Institute of Modern Physics, Chinese Academy of Sciences, Lanzhou 730000, People's Republic of China*

<sup>2</sup>*Flerov Laboratory of Nuclear Reactions, Joint Institute for Nuclear Research, RU-141980 Dubna, Russia*

<sup>3</sup>*School of Nuclear Science and Technology, University of Chinese Academy of Sciences, Beijing 100049, People's Republic of China*

<sup>4</sup>*School of Nuclear Science and Technology, Lanzhou University, Lanzhou 730000, People's Republic of China*

<sup>5</sup>*Guangxi Key Laboratory of Nuclear Physics and Technology, Guangxi Normal University, Guilin 541004, People's Republic of China*

<sup>6</sup>*Sino-French Institute of Nuclear Engineering and Technology, Sun Yat-Sen University, Zhuhai 519082, People's Republic of China*

<sup>7</sup>*Institute of Theoretical Physics, Chinese Academy of Sciences, Beijing 100190, People's Republic of China*

<sup>8</sup>*School of Physics Science and Engineering, Tongji University, Shanghai 200092, People's Republic of China*



(Received 20 September 2022; accepted 10 November 2022; published 12 December 2022)

The  $\alpha$  decays of  $^{207-209}\text{Ac}$ , located near the proton drip-line, were reinvestigated by means of  $\alpha$ -decay spectroscopy. They were produced in the fusion reaction  $^{36}\text{Ar} + ^{176}\text{Hf}$  and separated in flight using the gas-filled recoil separator SHANS. A new  $\alpha$ -decay line at 7483(15) keV was observed and assigned as the decay from the ground state of  $^{208}\text{Ac}$  to the excited ( $2^+$ ) or ( $4^+$ ) state in  $^{204}\text{Fr}$ . In addition, the previously known  $\alpha$ -decay properties of  $^{207-209}\text{Ac}$  were measured with improved precision. The half-lives obtained, together with the existing decay data of other  $N \leq 126$  actinium isotopes, were compared with the values calculated with the Wentzel-Kramers-Brillouin approximation and without considering the  $\alpha$ -preformation factors. It is shown that the calculated half-lives exhibit a distinct odd-even staggering (OES) following the same trend as the experimental data, whereas the amplitudes of the exhibited OES are 30–60 % of the real ones. This implies that apart from the  $\alpha$ -preformation factors, the  $\alpha$ -decay energies also contribute significantly to the OES of  $\alpha$ -decay half-lives.

DOI: [10.1103/PhysRevC.106.064311](https://doi.org/10.1103/PhysRevC.106.064311)

### I. INTRODUCTION

$\alpha$  decay is an important probe for studying heavy and superheavy nuclides, and the most significant quantities for  $\alpha$  decay are  $\alpha$ -decay energy  $Q_\alpha$ , partial half-life  $T_{1/2}^\alpha$ , and  $\alpha$ -preformation factor  $P_\alpha$  (or reduced  $\alpha$ -decay width). Interestingly, both  $T_{1/2}^\alpha$  and  $P_\alpha$  were found to exhibit odd-even staggering (OES) while changing neutron number [1–9]. The OES of  $\alpha$ -decay half-lives, i.e., an odd- $N$  isotope has a longer half-life than those of its even- $N$  neighbors, has long been known as a non-negligible effect in half-life calculations [4]. From the theoretical point of view, an estimate for the  $\alpha$ -decay half-life can be obtained through semiempirical Wentzel-Kramers-Brillouin (WKB) method, in which the  $\alpha$ -decay energy plays a crucial role in calculations. Nevertheless, since the  $Q_\alpha$  values are supposed to vary smoothly in the open-shell region, the OES of  $\alpha$ -decay half-lives is usually understood as

arising from the OES of  $\alpha$ -preformation factors, which itself is attributed to the blocking effect of unpaired nucleons [9]. We have recently pointed out that the  $\alpha$ -decay energies for nuclei with  $Z > 82$  and  $N < 126$  actually show regular and distinct OES (typical amplitude is about 70 keV) rather than the commonly supposed smooth pattern [10]. Given that the magnitude of  $T_{1/2}^\alpha$  is extremely sensitive to the  $Q_\alpha$  value, it is interesting to examine the effect of  $\alpha$ -decay energies on the OES in half-lives.

The nuclides in the region  $Z > 82$ ,  $N < 126$  are an ideal ground for studying the OES effects in  $\alpha$  decay, because their  $\alpha$  decays usually do not involve angular momentum transfers and behave quite regularly. However, due to the very fast decrease of the production cross sections with decreasing neutron number, the  $\alpha$ -decay properties of many nuclei close to the proton drip-line were determined with large uncertainties. To obtain precise experimental data, it is essential to restudy these nuclei with higher statistics. Furthermore, with the increase of statistics it is possible to obtain previously unknown information on nuclear structure, e.g., isomeric state and fine structure in  $\alpha$  decay [11–13].

\*zggan@impcas.ac.cn

†mxl@impcas.ac.cn

In this paper, we report on a detailed  $\alpha$ -decay study of  $^{207-209}\text{Ac}$  from the same experiment as in Ref. [10]. New and improved  $\alpha$ -decay data on these isotopes are obtained. By comparing the experimental half-lives of  $N \leq 126$  actinium isotopes with the values calculated using the WKB approximation, the impact of  $\alpha$ -decay energies on the OES of  $\alpha$ -decay half-lives is discussed for the first time.

## II. EXPERIMENTAL DETAILS

The  $^{207-209}\text{Ac}$  isotopes were produced in the fusion-evaporation reaction  $^{36}\text{Ar} + ^{176}\text{Hf}$ . The  $^{36}\text{Ar}^{11+}$  beam with energies of 197–199 MeV was provided by the Sector Focusing Cyclotron of the Heavy Ion Research Facility in Lanzhou (HIRFL), China. Three isotopically enriched (84.6%)  $^{176}\text{Hf}$  targets with thicknesses of 116–360  $\mu\text{g}/\text{cm}^2$  were mounted on a rocking frame which moves horizontally and periodically from side to side during irradiation. The average beam intensity was about 0.4  $\mu\text{A}$ , and the total irradiation time was 443 h.

The evaporation residues (ERs) recoiling out of the target were separated from the primary beam using the gas-filled Spectrometer for Heavy Atoms and Nuclear Structure (SHANS) [14], which was filled with helium gas at a pressure of 0.6 mbar. After passing through two multiwire proportional counters the residues were implanted into three 300- $\mu\text{m}$ -thick position-sensitive silicon strip detectors (PSSDs) installed side by side at the focal plane of the separator. Each PSSD, with an active area of  $50 \times 50 \text{ mm}^2$ , was divided into 16 vertical strips on the front side. Eight non-position-sensitive silicon detectors were mounted around and perpendicular to the PSSDs. They were used to measure  $\alpha$  particles escaping from the PSSDs. All the silicon detectors were cooled to a temperature of 251 K using circulating ethanol.

After amplified with preamplifiers, signals from all detectors were processed in a digital data acquisition system, in which the shapes of the signals from PSSDs were recorded in 30- $\mu\text{s}$ -long traces with 100 MHz sampling frequency. In the subsequent off-line data analysis, the time and energy information stored in the traces were extracted using the digital triangular algorithm [15] and pulse shape fitting method [16], respectively. Energy and position calibrations were performed using a three-peak external  $\alpha$  source ( $^{239}\text{Pu}$ ,  $^{241}\text{Am}$ , and  $^{244}\text{Cm}$ ) as well as the well-known peaks from nuclides produced in the  $^{36}\text{Ar} + ^{176}\text{Hf}$  reaction. The energy resolution [full width at half-maximum (FWHM)] of individual strips of PSSDs was about 35 keV for 6–10-MeV  $\alpha$  particles, and the vertical position resolution was better than 1.2 mm.

## III. RESULTS

To identify the nuclides of interest, a correlation analysis of the type ER- $\alpha_1$ - $\alpha_2$  was performed with a vertical position window of  $\pm 1.2$  mm and time windows of 0.9 s for the ER- $\alpha_1$  pair and 12 s for the  $\alpha_1$ - $\alpha_2$  pair. Here,  $\alpha_1$  means the  $\alpha$  decay of a parent nucleus and  $\alpha_2$  the one of a daughter nucleus. The results of the correlation analysis are shown in Fig. 1. Escaped events which did not deposit their full energies in the PSSD are excluded from the plot. The known radium isotopes

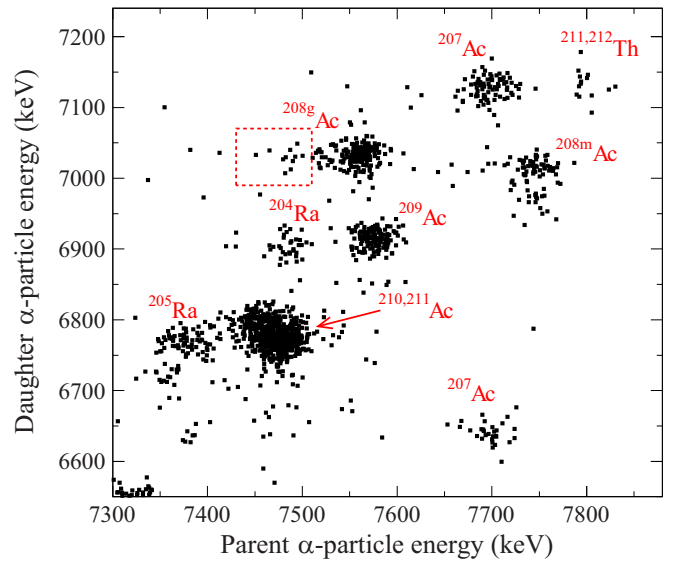


FIG. 1. Scatter plot showing the correlation between energies of parent and daughter  $\alpha$  decays in the reaction of  $^{36}\text{Ar} + ^{176}\text{Hf}$ . Maximum correlation times were 0.9 s for the ER- $\alpha_1$  pair and 12 s for the  $\alpha_1$ - $\alpha_2$  pair. Vertical position window was  $\pm 1.2$  mm. The dashed-line box indicates the location of the 11 events assigned to the new  $\alpha$ -decay branch of  $^{208g}\text{Ac}$ .

$^{204,205}\text{Ra}$  produced in the  $\alpha 4n$  and  $\alpha 3n$  evaporation channels, and the actinium isotopes  $^{207-209}\text{Ac}$  produced in the  $p4n$ ,  $p3n$ , and  $p2n$  channels are identified. The presence of  $^{211-212}\text{Th}$  and  $^{210-211}\text{Ac}$  can be explained by a small admixture of the heavier  $^{177-180}\text{Hf}$  isotopes in target material, as these nuclides are not expected to be produced at the selected beam energies on the  $^{176}\text{Hf}$  target. It is noteworthy that the event numbers of  $^{207-209}\text{Ac}$  observed in this experiment are significantly larger than those in earlier studies, which results in new and improved decay data.

### A. $\alpha$ decay of $^{208}\text{Ac}$

Prior to this work,  $^{208}\text{Ac}$  was only studied by Andreyev *et al.* [18] and Leino *et al.* [19] in 1994. In Ref. [18], an  $\alpha$  emitter with an  $\alpha$ -particle energy ( $E_\alpha$ ) of 7740(20) keV and a half-life of 50(20) ms was observed and tentatively assigned to  $^{208m}\text{Ac}$ . In Ref. [19], two  $\alpha$ -decaying states, with  $E_\alpha = 7572(15)$  keV and  $T_{1/2} = 95^{+24}_{-16}$  ms for the ( $3^+$ ) ground state and  $E_\alpha = 7758(20)$  keV and  $T_{1/2} = 25^{+9}_{-5}$  ms for the ( $10^-$ ) isomeric state, were identified in  $^{208}\text{Ac}$ . The numbers of decay events from  $^{208g}\text{Ac}$  and  $^{208m}\text{Ac}$  were  $\approx 30$  and 14, respectively.

In this work, a total of 202 correlated ER- $\alpha_1$ - $\alpha_2$  chains assigned to  $^{208g}\text{Ac}$  were found. The energy spectrum of  $^{208g}\text{Ac}$  shown in Fig. 2(a) can be recognized as having two  $\alpha$  peaks. The intense peak has an energy of 7561(14) keV, which is consistent with the previously reported ground-state to ground-state  $\alpha$  decay. The weak peak which contains 11 events has an energy of 7483(15) keV. The number of accidental ER- $\alpha_1$ - $\alpha_2$  sequences in the energy window defined by 7430–7510 keV and 6990–7070 keV (i.e., the dashed box

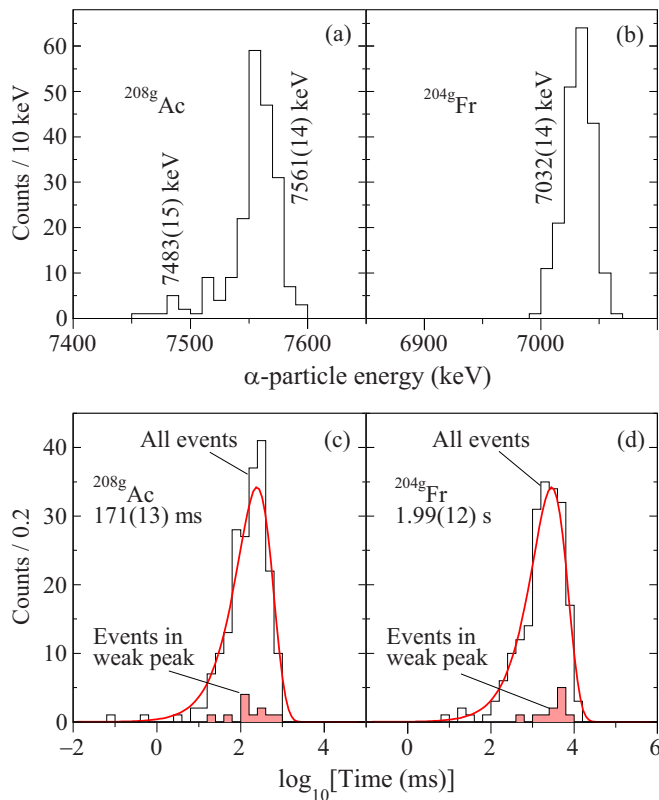


FIG. 2. (a)–(d) Energy and time distributions of the  $\alpha$  decays from  $^{208g}\text{Ac}$  and  $^{204g}\text{Fr}$ , respectively. The data were extracted from the decay chains  $\text{ER-}\alpha_1(^{208g}\text{Ac})\text{-}\alpha_2(^{204g}\text{Fr})$ . In (c) and (d), the events originating from the 7483-keV  $\alpha$  line are shown by full histograms. The red solid lines are the fitted decay curves according to Ref. [17].

area on Fig. 1) is estimated to be less than 0.2, and hence we attribute all the chains in the weak peak as real correlations. The time distribution of these events shown in Fig. 2(c) (full histogram) results in a half-life of  $168^{+72}_{-39}$  ms, which is approximately equal to the value of 170(13) ms for the 7561-keV events. Therefore, it is plausible to assume that the new  $\alpha$  line corresponds to the transition from  $^{208g}\text{Ac}$  to a low-lying level of  $^{204}\text{Fr}$ . In analogy to the  $\alpha$  decay of  $^{204}\text{Fr}$  [20], we assign the 7483-keV  $\alpha$  line as the decay from the ground state of  $^{208}\text{Ac}$  to the excited ( $2^+$ ) or ( $4^+$ ) state in  $^{204}\text{Fr}$ . From the number of observed events, the branching ratios of  $\alpha$  decay to ground and excited states are estimated to be  $<95\%$  and  $>5\%$  (see below), respectively. Note that these values are deduced without considering the  $\beta$ -decay branch of  $^{208}\text{Ac}$ . On the basis of all correlation chains, a half-life of 171(13) ms is deduced for  $^{208g}\text{Ac}$ , which is somewhat different from the previously reported  $95^{+24}_{-16}$  ms [19]. In addition, the  $\alpha$ -particle energy and half-life of the daughter nuclide  $^{204g}\text{Fr}$  are determined to be 7032(14) keV and 1.99(12) s [see Figs. 2(b) and 2(d)], which agree well with the literature values reported in Refs. [20,21]. According to the energy difference between the 7561-keV and 7483-keV transitions, the excitation energy of the ( $2^+$ ) or ( $4^+$ ) level in  $^{204}\text{Fr}$  is determined to be 80(5) keV. Due to the small excitation energy, the internal conversions associated with the 80-keV transition would be highly favored. The total

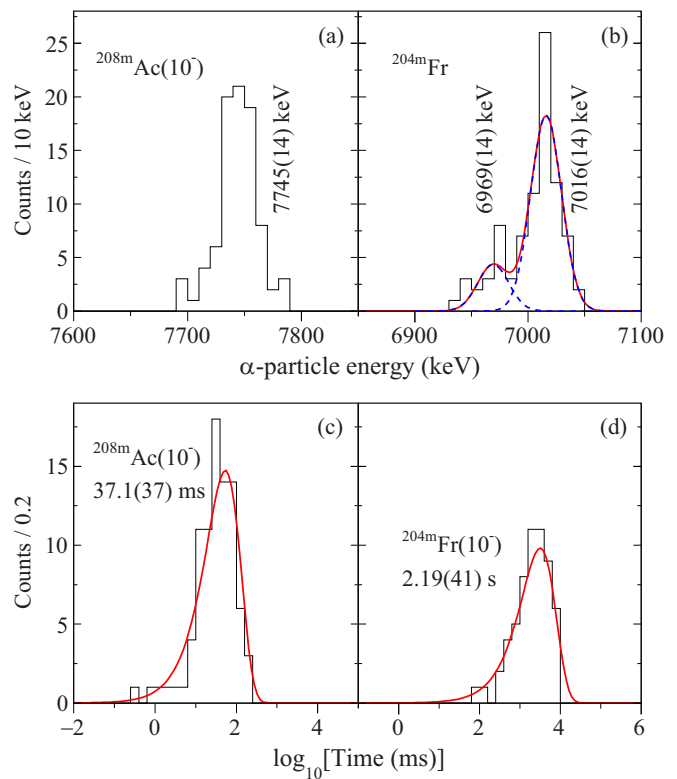


FIG. 3. (a)–(d) Energy and time distributions of the  $\alpha$  decays from  $^{208m}\text{Ac}$  and  $^{204m}\text{Fr}$ , respectively. The data were extracted from the decay chains  $\text{ER-}\alpha_1(^{208m}\text{Ac})\text{-}\alpha_2(^{204m}\text{Fr})$ . See text for details.

conversion coefficients for  $M1$  and  $E2$  transitions calculated using BRICC code [22] are 5.39 and 25.1, respectively. Since the excitation energy is lower than the  $K$  binding energy of  $\text{Fr}$  (101.15 keV), the ( $2^+$ ) or ( $4^+$ ) state mainly decays into the ground state by  $L$  conversion. The sum energy of 7483-keV  $\alpha$  particle and full-energy  $L$ -conversion electron (61.5 keV) will be close to the energy of the main peak. It thus cannot be excluded that some events counted as main peak are in fact the sums of 7483-keV  $\alpha$  particles and conversion electrons.

As for  $^{208m}\text{Ac}$  ( $10^-$ ), a total of 87  $\alpha$ -decay chains were detected. From the energy and time distributions of these events, an improved  $\alpha$ -particle energy of 7745(14) keV and a more precise half-life of 37.1(37) ms are deduced as shown in Figs. 3(a) and 3(c). The energy spectrum of the daughter  $^{204m}\text{Fr}$  is shown in Fig. 3(b). It is evident that there are two peaks close to each other. A sum of two Gaussian functions is used to fit the peaks, which results in the observation of two  $\alpha$ -particle energies of 7016(14) keV and 6969(14) keV. The 7016-keV and 6969-keV  $\alpha$  lines are consistent with the  $\alpha$  decays of ( $10^-$ ) and ( $7^+$ ) isomeric states, respectively. The correlation observed between the  $\alpha$  decays of  $^{208m}\text{Ac}$  ( $10^-$ ) and  $^{204m}\text{Fr}$  ( $7^+$ ) confirms the  $E3$  internal transition between the ( $10^-$ ) and ( $7^+$ ) states in  $^{204}\text{Fr}$  [23]. Unfortunately, due to the high detection threshold of about 0.35 MeV, we did not observe the correlation between  $\alpha$  decay and internal conversion electron. Assuming the  $\alpha$ -decay branch of the ( $7^+$ ) state in  $^{204}\text{Fr}$  is 100%, the  $\alpha$ -decay branch of the ( $10^-$ ) state is determined to be 80(7)%, which is consistent with the value of

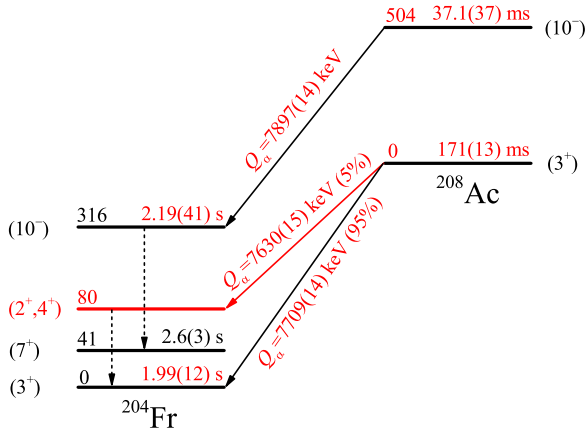


FIG. 4. Proposed  $\alpha$ -decay scheme of  $^{208}\text{Ac}$ . Level energies are given in keV. The  $Q_\alpha$  values were deduced using the relation  $Q_\alpha = (1 + m_\alpha/m_d) \times E_\alpha$ , where  $m_\alpha$  and  $m_d$  are the masses of  $\alpha$  particle and daughter nucleus, respectively. The new level and improved data measured in this work are marked in red color. The literature values are taken from [21,26].

74(8)% reported in Ref. [24] but disagrees with the value of 53(10)% from Ref. [25]. From the time differences between  $\alpha_1$  and  $\alpha_2$  (limited to 7000–7050 keV) decays, the half-life of  $^{204m}\text{Fr}$  ( $10^-$ ) is deduced to be 2.19(41) s [see Fig. 3(d)], which is slightly larger than the literature value 1.65(15) s [26]. The production cross section of  $^{208}\text{Ac}$  is estimated to be 2.26(14) nb. Based on the above results, we propose an updated decay scheme of  $^{208}\text{Ac}$  shown in Fig. 4.

### B. $\alpha$ decays of $^{207}\text{Ac}$ and $^{209}\text{Ac}$

The isotope  $^{207}\text{Ac}$  was first reported, together with  $^{208}\text{Ac}$ , in Ref. [19]. It was produced in the  $8n$  evaporation channel of the fusion reaction  $^{40}\text{Ar} + ^{175}\text{Lu}$  and identified by observing two  $\alpha$ -decay events. Later another nine decay events of  $^{207}\text{Ac}$  were observed by Eskola *et al.* [27] in the reaction  $^{36}\text{Ar} + ^{175}\text{Lu}$ . Taking into account all the 11 events, the  $\alpha$ -decay properties of  $^{207}\text{Ac}$  were determined to be  $E_\alpha = 7693(25)$  keV and  $T_{1/2} = 27_{-6}^{+11}$  ms, which have been adopted as tabulated data for more than 20 years. In this work, altogether 154 chains of the type ER- $\alpha_1$ - $\alpha_2$  assigned to  $^{207}\text{Ac}$  were observed. The energy and time distributions displayed in Figs. 5(a) and 5(c) give an improved  $\alpha$ -particle energy of 7700(14) keV and a more precise half-life of 36.5(27) ms, which are in agreement with the previously reported data. The production cross section of  $^{207}\text{Ac}$  is estimated to be 1.2(1) nb. The first study of  $^{209}\text{Ac}$  was performed by Valli *et al.* [28] who produced it by the  $^{20}\text{Ne} + ^{197}\text{Au}$  reaction. The identification of  $^{209}\text{Ac}$  was based on excitation function measurements, and its  $\alpha$ -decay properties were measured to be  $E_\alpha = 7585(15)$  keV and  $T_{1/2} = 100(50)$  ms. These results were later confirmed by Andreyev *et al.* [ $E_\alpha = 7590(20)$  keV,  $T_{1/2} = 80(30)$  ms] [18], Leino *et al.* [ $E_\alpha = 7581(15)$  keV,  $T_{1/2} = 91_{-14}^{+21}$  ms] [19], Heßberger *et al.* [ $E_\alpha = 7577(10)$  keV,  $T_{1/2} = 98_{-27}^{+59}$  ms] [29], and Yang *et al.* [ $E_\alpha = 7575(23)$  keV,  $T_{1/2} = 98(22)$  ms] [30]. In the present work, 181  $\alpha$ -decay events of  $^{209}\text{Ac}$  were clearly identified. Based on these events, an  $\alpha$ -particle energy of

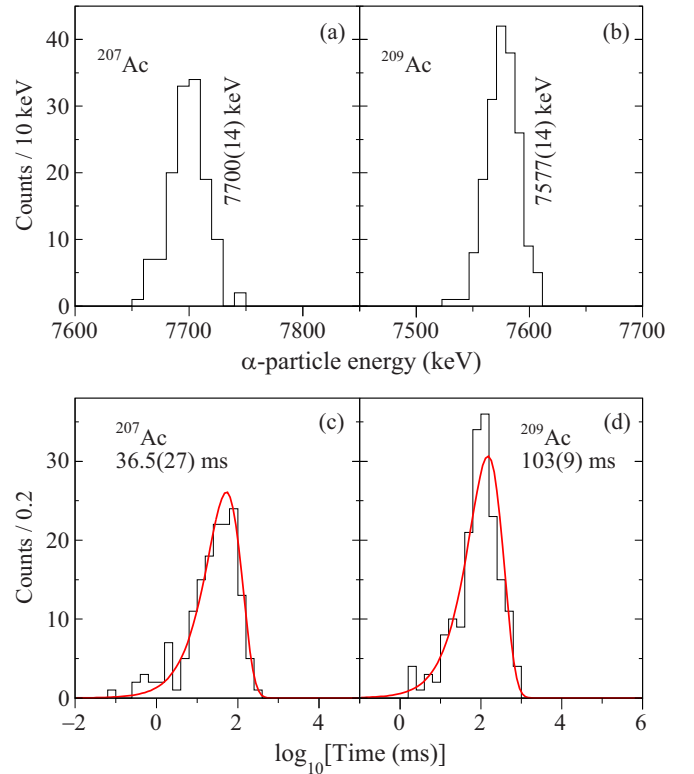


FIG. 5. (a)–(d) Energy and time distributions of the  $\alpha$  decays from  $^{207}\text{Ac}$  and  $^{209}\text{Ac}$ , respectively.

7576(14) keV and a half-life of 103(9) ms are deduced [see Figs. 5(b) and 5(d)], which are compatible with the previously reported values.

## IV. DISCUSSION

Figures 6(a) and 6(b) present the systematics of the experimental  $Q_\alpha$  and  $\log_{10}T_{1/2}^\alpha$  (logarithm of partial half-life) values of  $N \leq 126$  actinium isotopes, respectively. It can be seen that the newly measured  $\alpha$ -decay data of  $^{207-209}\text{Ac}$  (hollow squares) fit well into the systematics, where both  $Q_\alpha$  and  $T_{1/2}^\alpha$  exhibit obvious OES along the isotopic chain. For instance, the  $\alpha$ -decay energy of  $^{208}\text{Ac}$  is smaller than those of  $^{207}\text{Ac}$  and  $^{209}\text{Ac}$ , whereas its half-life is longer than those of the two neighbors. Previously, the effect of  $\alpha$ -decay energies on the OES in half-lives was rarely discussed due to the neglect of the OES in  $Q_\alpha$  values. We expect that the distinct odd-even effect in  $Q_\alpha$  values shown in Fig. 6(a) should play an important role in the occurrence of the OES in half-lives. To examine this speculation, we first need to calculate the  $\alpha$ -decay half-lives of actinium isotopes based on experimental  $Q_\alpha$  values.

Within the Gamow picture [32], the  $\alpha$ -decay is considered as a quantum tunneling process of a preformed  $\alpha$  particle penetrating the potential barrier. Accordingly, the  $\alpha$ -decay half-life is expressed by

$$T_{1/2}^\alpha = \frac{\ln 2}{P_\alpha \nu P}, \quad (1)$$

where  $\nu$  and  $P$  denote the assault frequency and penetration probability, respectively. Since the  $\nu$  is almost constant in

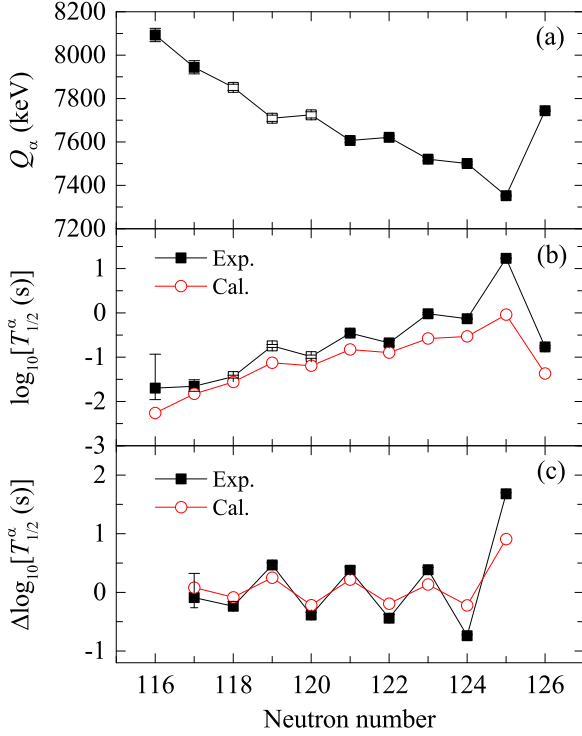


FIG. 6. (a) The  $Q_\alpha$  values measured in this work (hollow squares) compared to the systematics of ground-state to ground-state transitions for neutron-deficient actinium isotopes. (b) Comparison of the experimental  $\alpha$ -decay half-lives of actinium isotopes (squares) with the calculated values (circles). The literature values are taken from [31]. (c) Comparison of experimental and calculated OES of half-lives. See text for details.

the open-shell region,  $P_\alpha$  and  $P$  are the main varying components of half-life. The penetration probability  $P$  is usually obtained using WKB approximation and thus depends closely on the choice of interaction potential and the corresponding  $Q_\alpha$  value. Here, the penetration probabilities were calculated using the formalism of Rasmussen [33] assuming  $L = 0$  transitions,  $P_\alpha$  was chosen as 1, and  $\nu$  was taken to be equal to that of  $^{212}\text{Po}$ . The results of the calculations are compared with experimental data in Fig. 6(b). As expected, the calculated half-lives exhibit distinct OES along the isotopic chain, though they are systematically shorter than the experimental half-lives. The deviation is understandable as the omission of the variation of  $\alpha$ -preformation factors. Since the effective potential between the  $\alpha$  particle and daughter nucleus does not give rise to odd-even differences, the OES observed in the calculated half-lives is only caused by the OES of  $\alpha$ -decay energies.

To compare the calculated OES with the experimental one, a three-point indicator [10] defined as

$$\Delta \log_{10} T_{1/2}^\alpha(N) = \frac{1}{2} [2 \log_{10} T_{1/2}^\alpha(N) - \log_{10} T_{1/2}^\alpha(N-1) - \log_{10} T_{1/2}^\alpha(N+1)] \quad (2)$$

is used. Values of the  $\Delta \log_{10} T_{1/2}^\alpha$  are shown in Fig. 6(c) where we compare experimental data with those extracted from the calculated  $T_{1/2}^\alpha$  values. We note that the calculated staggering

trend is consistent with the experimental one, but the amplitude values are 30–60 % of the real ones. Similar situations can also be seen in other neutron-deficient Po-U isotopes with a few exceptions. This indicates that, at least in the nuclear region of  $Z > 82$  and  $N < 126$ , the  $\alpha$ -decay energies make a significant contribution to the occurrence of the OES in half-lives. Meanwhile, it also implies that, in addition to the OES of  $\alpha$ -decay energies, another odd-even contribution arising from the  $\alpha$ -preformation factors is needed to fully reproduce the OES in half-lives.

In fact, the impact of  $\alpha$ -decay energies on the OES of half-lives can also be examined through the simple linear relationship between  $\log_{10} T_{1/2}^\alpha$  and  $Q_\alpha^{-1/2}$  in the Geiger-Nuttall law or other empirical formulas [34], which will give almost the same results as the WKB approximation. The OES effect of half-lives is usually taken into account in empirical formulas by giving different sets of coefficients for different  $\alpha$ -decay cases or by adding odd-even terms. It now appears that these operations are only related to the contribution of  $\alpha$ -preformation factors.

## V. SUMMARY

In conclusion, the  $\alpha$  decays of  $^{207-209}\text{Ac}$  have been restudied with increased statistics. A new  $\alpha$ -decay branch with energy of 7483(15) keV was found in  $^{208}\text{Ac}$  and assigned to the transition from the ground state to the excited ( $2^+$ ) or ( $4^+$ ) state in the daughter nucleus  $^{204}\text{Fr}$ . In addition, the known  $\alpha$ -decay properties of  $^{207-209}\text{Ac}$  were measured with improved precision. The obtained  $\alpha$ -decay energies and half-lives of  $^{207-209}\text{Ac}$  fit well into the systematics with obvious OES. To examine the effect of  $\alpha$ -decay energies on the OES in half-lives, we calculated the half-lives of  $^{205-215}\text{Ac}$  using the WKB approximation. From a comparison with the experimental data, it is found that the OES effect of  $\alpha$ -decay half-lives comes from both  $\alpha$ -decay energies and  $\alpha$ -preformation factors.

## ACKNOWLEDGMENTS

We thank the HIRFL staff for providing the stable and high-intensity  $^{36}\text{Ar}$  beam. We also thank H.-F. Zhang for helpful discussion on the  $\alpha$ -decay half-life calculation. This work was partially supported by the National Key R&D Program of China (Contract No. 2018YFA0404402), the Strategic Priority Research Program of Chinese Academy of Sciences (Grant No. XDB34010000), the National Natural Science Foundation of China (Grants No. U1932139, No. 11975279, No. 12105328, No. 12075286, No. 11961141004, No. 11965003, No. 12135004, and No. 11635003), the Key Research Program of the Chinese Academy of Sciences (Grant No. ZDBS-LY-SLH017), the Guangdong Major Project of Basic and Applied Basic Research (Grant No. 2021B0301030006), the Youth Innovation Promotion Association CAS (Grant No. 2020409), the CAS Project for Young Scientists in Basic Research (Grant No. YSBR-002), the Special Research Assistant Project of the Chinese Academy of Sciences, and the CAS Scholarship.

- [1] C. Xu and Z. Ren, *Nucl. Phys. A* **760**, 303 (2005).
- [2] C. Xu and Z. Ren, *Phys. Rev. C* **76**, 027303 (2007).
- [3] W. M. Seif, *Phys. Rev. C* **91**, 014322 (2015).
- [4] J.-G. Deng, H.-F. Zhang, and G. Royer, *Phys. Rev. C* **101**, 034307 (2020).
- [5] J.-G. Deng and H.-F. Zhang, *Phys. Rev. C* **102**, 044314 (2020).
- [6] J.-G. Deng and H.-F. Zhang, *Phys. Lett. B* **816**, 136247 (2021).
- [7] Y. Qian and Z. Ren, *Nucl. Phys. A* **852**, 82 (2011).
- [8] Y. Ren and Z. Ren, *Nucl. Sci and Tech.* **24**, 050518 (2013).
- [9] X.-D. Sun, C. Duan, J.-G. Deng, P. Guo, and X.-H. Li, *Phys. Rev. C* **95**, 014319 (2017).
- [10] H. B. Yang, Z. G. Gan, Z. Y. Zhang, M. H. Huang, L. Ma, M. M. Zhang, C. X. Yuan, Y. F. Niu, C. L. Yang, Y. L. Tian, L. Guo, Y. S. Wang, J. G. Wang, H. B. Zhou, X. J. Wen, H. R. Yang, X. H. Zhou, Y. H. Zhang, W. X. Huang, Z. Liu *et al.*, *Phys. Rev. C* **105**, L051302 (2022).
- [11] M. M. Zhang, H. B. Yang, Z. G. Gan, Z. Y. Zhang, M. H. Huang, L. Ma, C. L. Yang, C. X. Yuan, Y. S. Wang, Y. L. Tian, H. B. Zhou, S. Huang, X. T. He, S. Y. Wang, W. Z. Xu, H. W. Li, X. X. Xu, J. G. Wang, H. R. Yang, L. M. Duan *et al.*, *Phys. Lett. B* **800**, 135102 (2020).
- [12] L. Ma, Z. Y. Zhang, H. B. Yang, M. H. Huang, M. M. Zhang, Y. L. Tian, C. L. Yang, Y. S. Wang, Z. Zhao, W. X. Huang, Z. Liu, X. H. Zhou, and Z. G. Gan, *Phys. Rev. C* **104**, 044310 (2021).
- [13] M. M. Zhang, Y. L. Tian, Y. S. Wang, X. H. Zhou, Z. Y. Zhang, H. B. Yang, M. H. Huang, L. Ma, C. L. Yang, Z. G. Gan, J. G. Wang, H. B. Zhou, S. Huang, X. T. He, S. Y. Wang, W. Z. Xu, H. W. Li, X. X. Xu, L. M. Duan, Z. Z. Ren *et al.*, *Phys. Rev. C* **100**, 064317 (2019).
- [14] Z. Y. Zhang, L. Ma, Z. G. Gan, M. H. Huang, T. H. Huang, G. S. Li, X. L. Wu, G. B. Jia, L. Yu, H. B. Yang, Z. Y. Sun, X. H. Zhou, H. S. Xu, and W. L. Zhan, *Nucl. Instrum. Methods Phys. Res. B* **317**, 315 (2013).
- [15] Valentin T. Jordanov and Glenn F. Knoll, *Nucl. Instrum. Methods Phys. Res. A* **345**, 337 (1994).
- [16] H. B. Yang, Z. G. Gan, Z. Y. Zhang, M. M. Zhang, M. H. Huang, L. Ma, and C. L. Yang, *Eur. Phys. J. A* **55**, 8 (2019).
- [17] K. H. Schmidt, *Eur. Phys. J. A* **8**, 141 (2000).
- [18] A. N. Andreyev, D. D. Bogdanov, V. I. Chepigin, A. P. Kabachenko, O. N. Malyshev, Yu. A. Muzychka, B. I. Pustynnik, G. M. Ter-Akopian, and A. V. Yeremin, *Nucl. Phys. A* **568**, 323 (1994).
- [19] M. Leino, J. Uusitalo, T. Enqvist, K. Eskola, A. Jokinen, K. Loberg, W. H. Trzaska, and J. Äystö, *Z. Phys. A* **348**, 151 (1994).
- [20] M. Huyse, P. Decrock, P. Dendooven, G. Reusen, P. Van Duppen, and J. Wauters, *Phys. Rev. C* **46**, 1209 (1992).
- [21] J. Uusitalo, M. Leino, T. Enqvist, K. Eskola, T. Grahn, P. T. Greenlees, P. Jones, R. Julin, S. Juutinen, A. Keenan, H. Kettunen, H. Koivisto, P. Kuusiniemi, A.-P. Leppänen, P. Nieminen, J. Pakarinen, P. Rahkila, and C. Scholey, *Phys. Rev. C* **71**, 024306 (2005).
- [22] T. Kibédi, Jr., T. W. Burrows, M. B. Trzhaskovskaya, P. M. Davidson, and C. W. Nestor, *Nucl. Instrum. Methods Phys. Res. A* **589**, 202 (2008).
- [23] U. Jakobsson, J. Uusitalo, S. Juutinen, M. Leino, T. Enqvist, P. T. Greenlees, K. Hauschild, P. Jones, R. Julin, S. Ketelhut, P. Kuusiniemi, M. Nyman, P. Peura, P. Rahkila, P. Ruotsalainen, J. Sarén, C. Scholey, and J. Sorri, *Phys. Rev. C* **85**, 014309 (2012).
- [24] C. R. Bingham, J. D. Richards, B. E. Zimmerman *et al.*, *International Conference on Exotic Nuclei and Atomic Masses (ENAM 95)* (Editions Frontieres, France, 1995), pp. 545–546.
- [25] K. M. Lynch, Laser assisted nuclear decay spectroscopy: A new method for studying neutron-deficient francium, Ph.D. thesis, The University of Manchester, 2013.
- [26] U. Jakobsson, S. Juutinen, J. Uusitalo, M. Leino, K. Auranen, T. Enqvist, P. T. Greenlees, K. Hauschild, P. Jones, R. Julin, S. Ketelhut, P. Kuusiniemi, M. Nyman, P. Peura, P. Rahkila, P. Ruotsalainen, J. Sarén, C. Scholey, and J. Sorri, *Phys. Rev. C* **87**, 054320 (2013).
- [27] K. Eskola, P. Kuusiniemi, M. Leino, J. F. C. Cocks, T. Enqvist, S. Hurskanen, H. Kettunen, W. H. Trzaska, J. Uusitalo, R. G. Allatt, P. T. Greenlees, and R. D. Page, *Phys. Rev. C* **57**, 417 (1998).
- [28] Kalevi Valli, William J. Treytl, and Earl K. Hyde, *Phys. Rev.* **167**, 1094 (1968).
- [29] F. P. Heßberger, S. Hofmann, D. Ackermann, V. Ninov, M. Leino, S. Saro, A. Andreyev, A. Lavrentev, A. G. Popeko, and A. V. Yeremin, *Eur. Phys. J. A* **8**, 521 (2000).
- [30] H. Yang, L. Ma, Z. Zhang, L. Yu, G. Jia, M. Huang, Z. Gan, T. Huang, G. Li, X. Wu, Y. Fang, Z. Wang, B. Gao, and W. Hua, *J. Phys. G: Nucl. Part. Phys.* **41**, 105104 (2014).
- [31] National Nuclear Data Center, <https://www.nndc.bnl.gov/>, accessed March 2, 2022.
- [32] G. Gamow, *Z. Phys.* **51**, 204 (1928).
- [33] John O. Rasmussen, *Phys. Rev.* **113**, 1593 (1959).
- [34] H. C. Manjunatha, L. Seenappa, and K. N. Sridhar, *Eur. Phys. J. Plus* **134**, 477 (2019).